A Novel Differential Microstrip Patch Antenna and Array at 79 GHz

#Z. Tong[1], A. Stelzer[1,2], C. Wagner[2], R. Feger[2], E. Kolmhofer[3]
[1]Institute for Communications & Information Engineering, Johannes Kepler University
Altenberger Str. 69, A-4040 Linz, Austria, {z.tong, c.wagner, r.feger, a.stelzer}@icie.jku.at
[2]Christian Doppler Laboratory for Integrated Radar Sensors, Johannes Kepler University
Altenberger Str. 69, A-4040 Linz Austria
[3]DICE GmbH & Co KG
Freistaedter Strasse 400, 4040 Linz, Austria, erich.kolmhofer@infineon.com

Abstract

A novel differential microstrip patch antenna (DMPA) is designed for autonomous cruise control radar systems at 79 GHz. Distinct from conventional single-ended patch antennas, the DMPA uses a pair of coupled lines as feeding line. It eliminates the need of a balun in the RF frontend and supports the realization of more compact radar frontend. First, a single DMPA is designed. The impedance bandwidth reaches 4.7 GHz and the gain at 79 GHz is 6.2 dBi. Simulations show that the length of the patch determines the resonance frequency and the gap between the feed points affects the patch impedance. Furthermore, a four-element series-fed array is presented with 4.6 GHz bandwidth and 12.8 dBi gain. Both the single DMPA and the four-element DMPA array were fabricated and measured. Measurement results show good agreement with simulation results.

1. Introduction

Differential circuits are used in silicon MMICs [1]. Unfortunately most of the conventional antennas are of single-ended type. Therefore at least a balun is needed between the differential circuits and the single-ended antenna/array. Research on differential antennas has become more and more attractive recently [2, 3]. These differential antennas use either proximity coupled structures or probe feed structures and frequency ranges are below 10 GHz. In this paper, a novel differential microstrip patch antenna/array (DMPA) for autonomous cruise control (ACC) applications at 79 GHz is presented. For this frequency range, to the authors' knowledge, it is the first time that a fully differential microstrip antenna/array is presented. The novel DMPA eliminates not only the loss dure to a balun, it also inherits significant advantages from the microstrip line structures, such as low profile, compact size, low cost, simple fabrication, etc.

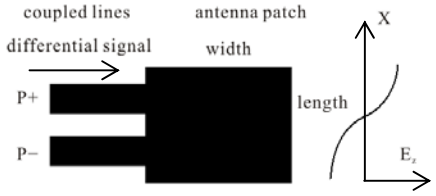

Fig. 1. Structure of a single DMPA and the E-field.

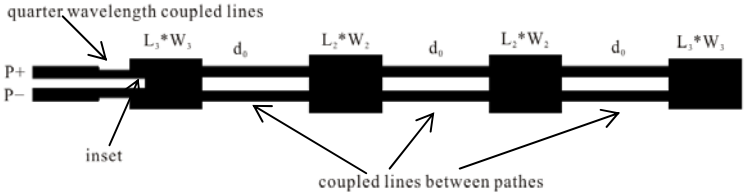

Fig. 2. A four-element series-fed DMPA array.

The structure of a single DMPA and the E-field are shown in Fig. 1. It consists of the radiation part-antenna patch and the feeding part-coupled lines. Through the feeding line, the differential signals are injected into the non-radiant edge of the antenna patch (left side of Fig. 1, the positive port is denoted by P+, the negative port by P-). The electric field of the patch is shown on the right side of Fig. 1. The Z direction is perpendicular to the antenna plane. The length of the patch determines the resonance

frequency of the patch, the distance between the feeding points (centers of the coupled lines) determines the impedance of the patch. A more detailed discussion on this topic is given in Section 2.

At first, a single DMPA is presented. Later on, a four-element series-fed DMPA array was also designed (see Fig. 2). Four antenna patches are connected by the coupled lines. A matching network at the first patch was used for the impedance match of the antenna array. Both antenna and array were fabricated on Taconic TLE-95 and measured.

2. Design Procedure

In this section the design rules for a single DMPA and a four-element series-fed DMPA array at 79 GHz are discussed. The design procedure of the single DMPA includes two steps. In the first step, the dimension of the patch can be calculated according to [4]. The width of a single patch is given by

$$W = \frac{c}{2 f_{\mathrm{r}}} \sqrt{\frac{2}{\varepsilon_{\mathrm{r}} + 1}} \tag{1}$$

with c as the free-space velocity of light, ε_{r} (= 3) as the relative permittivity, and f_{r} as the resonance frequency. The length L of a single patch is calculated to

$$L = \frac{1}{2}\lambda_{\mathrm{r}} - 2\Delta l \tag{2}$$

$$\frac{\Delta l}{h} = 0.412 \frac{(\varepsilon_{\mathrm{eff}} + 0.3)\left(\frac{W}{h} + 0.264\right)}{(\varepsilon_{\mathrm{eff}} - 0.258)\left(\frac{W}{h} + 0.8\right)} \tag{3}$$

with $\varepsilon_{\mathrm{eff}}$ as the effective permittivity, λ_{r} as the relative wavelength. They can be calculated according to [4]. In (3), h (= 0.127 mm) is the height of the substrate. The patch parameters are calculated as following: L_1 = 0.98 mm and W_1 = 1.34 mm. The loci of the patch impedance in the Smith chart is approximately a circle with constant conductance (see Fig. 3), but the center is shifted to the upper part. The patch impedance is determined by the feeding positions. With increasing the spacing (s_n) between the feeding points, the patch impedance at 79 GHz increases rapidly (see Fig. 3). If the feeding points are located too close to one another ($s_n < 0.1\ \lambda_0$), the patch resonance will disappear. Therefore, the second step is to optimize the patch impedance. With a 3D EM simulator, a single DMPA was design for 100 Ohm differential impedance. Simulation results show an impedance bandwidth of 3.1 GHz and 6.1 dBi antenna gain at a frequency of 79 GHz.

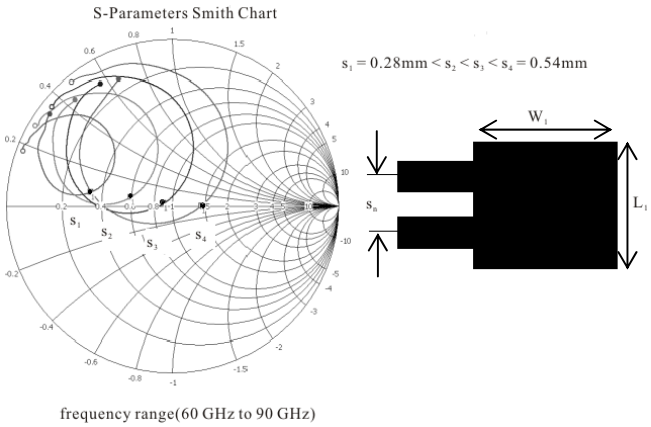

Fig. 3. Patch impedance with different feeding points distances.

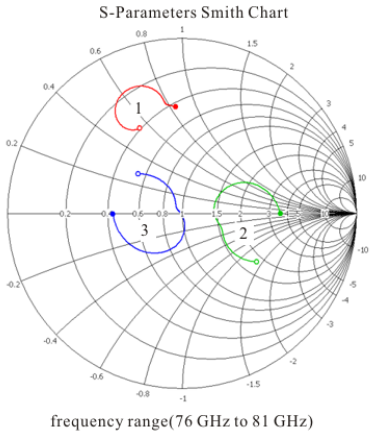

Fig. 4. Matching network function.

Starting from the dimension of a single DMPA, it is possible to extend to a four-element series-fed array (see Fig. 2). The antenna array is composed of four antenna patches, which are connected by a pair of coupled lines in between. The design of an antenna array is more complicated than of a single patch antenna. Besides the impedance match, the radiation pattern is another important factor to be considered. The distance between the antenna patches (center to center) is a critical parameter influencing the radiation pattern. It equals the sum of the width of the patch (W) and the gap between the antenna patches (d_0). In order to keep each antenna patch radiating in phase at the center frequency, a distance of 3.48 mm (0.92 λ_0) is used.

Compared to the single DMPA, the series-fed DMPA array introduces more inductance in the antenna impedance. A matching network is designed between antenna patches and feed line. The matching network consists of an inset on the first patch and quarter wavelength coupled lines. The inset works as a section of transmission line, it converts the antenna impedance from inductive part in Smith Chart (curve 1 in Fig. 4) to the high resistance part of real axis (curve 2). Then the quarter wavelength transforms the antenna impedance to 100 Ohm differential impedance.

Based on simulation, a four-element series-fed antenna array is realized with following dimensions: d_0 = 2.08 mm, L_2 = 1.1 mm, L_3 = 0.96 mm and $W_2 = W_3$ = 1.4 mm. The total length of the array is 11.84 mm (without the matching network). The impedance bandwidth, derived from simulation results, is 4.1 GHz and the antenna gain is 12.0 dBi, respectively.

3. Measurement

Both, the single patch antenna as well as the array, were fabricated and measured. For the S-parameter measurement, it is difficult to get one-port differential S-parameters directly. Therefore, the antenna/array is measured as a single-ended two-port device at first. Then, the differential S-parameters are calculated by using the following matrix conversion [5]:

$$\mathbf{M} = \frac{1}{\sqrt{2}}\begin{bmatrix} 1 & -1 \\ 1 & 1 \end{bmatrix} \tag{4}$$

$$\mathbf{S}_{\mathrm{dm}} = \mathbf{M} \cdot \mathbf{S} \cdot \mathbf{M} \tag{5}$$

with $\mathbf{S}$ as the measured single-ended two-port S-parameters and $\mathbf{S}_{\mathrm{dm}}$ as the calculated one-port differential S-parameters.

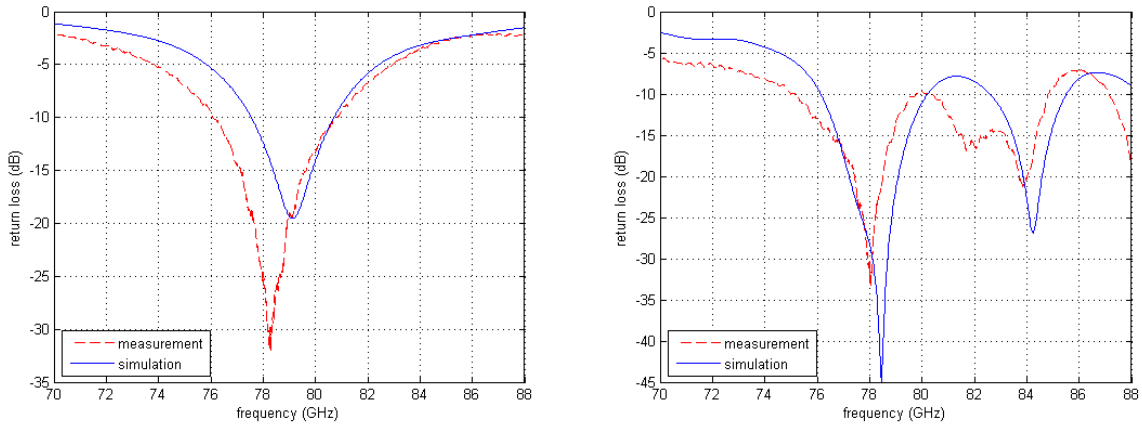

Fig. 5. Measured and simulated return loss of a single DMPA (a) and of a four-element DMPA array (b).

Figure 5 shows the measurements in comparison with the simulation results of the return loss of the two antennas. The measured bandwidth of a single DMPA is 4.7 GHz, that of a four-element series-

fed DMPA array is 4.6 GHz respectively. The bandwidths of the measurement results are wider than the simulation results. This is possible because of the losses in the substrates.

During the far field measurements, a waveguide to differential microstrip line transition was used (see Fig. 6). The waveguide signal is injected from the back of the transition and converted to a differential signal through the transition. A short end cap with an open channel is placed on the top of the transition. The differential antenna/array can be connected to the output of the transition directly. The measurement setup is shown in Fig. 7.

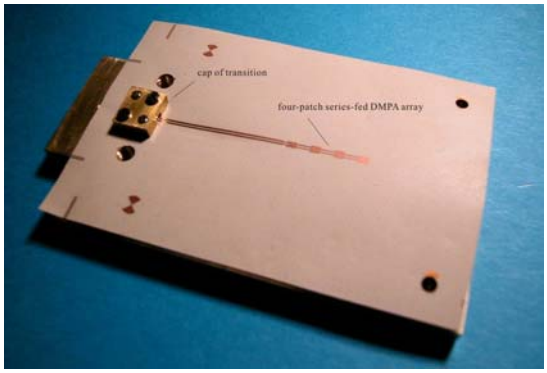

Fig. 6. Photograph of the transition and four-element series-fed DMPA array.

Fig. 7. Photograph of the far field measurement setup.

The normalized E-plane and H-plane, co-polarization and cross-polarization radiation patterns of both antennas are plotted in Fig. 8 and Fig. 9. The simulation results of the cross-polarization in H-plane are neglected here because of its quite low level.

There were additional noises observed within the far field measurements. Therefore average values (20 samples per degree) were used for plotting the results. Because of the height of the transition cap, the last several degrees of the radiation patterns in the H-plane (85~90 degree) are disturbed.

Within the far field measurements, some ripples were observed in the radiation pattern, stronger in the E-plane than in the H-plane, stronger for the single patch antenna than the antenna array. Radiation from the surface wave at the edges of PCBs could be the most likely explanation. Absorbing material was used on the edges of PCBs. This reduced some surface wave effects, but also distorted radiation patterns at the angle ranges ±80~90 degree.

The gain of the antenna/array at 79 GHz is also measured. The calibrated gain for the single DMPA is 6.2 dBi and 12.8 dBi for the four-element array, respectively.

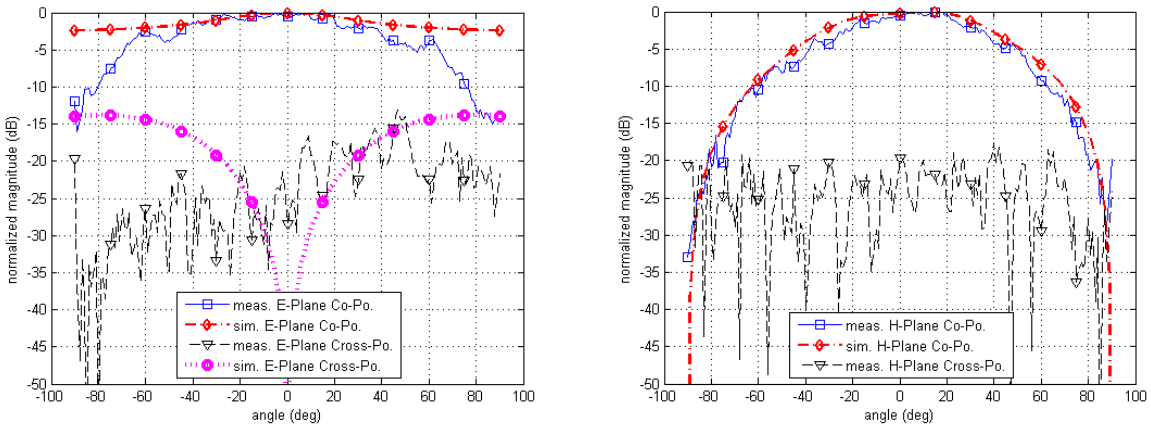

(a) (b)

Fig. 8. Normalized radiation pattern of a single DMPA for E-plane (a) and H-plane (b).

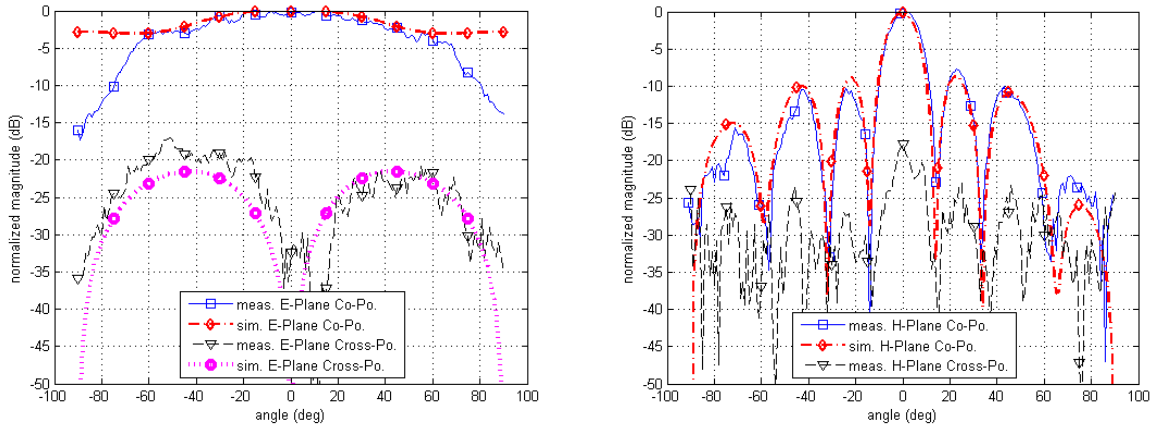

(a) (b)

Fig. 9. Normalized radiation pattern of a four-element DMPA array of E-plane (a) and H-plane (b).

4. Conclusions

In this paper, a novel DMPA and a four-element series-fed DMPA array are presented. These DMPAs may be integrated with differential circuits easily. They can support more compact RF frontend size and reduce the loss of the balun. The general design rules of the single patch antenna and the antenna array are illustrated also.

Both the single patch antenna as well as the antenna array were fabricated and measured. The measured results agree well with simulated results.

Within far field measurements, radiation of surface waves is observed. Removing the influence from the surface waves radiation is one of the goals for the further design.

Acknowledgments

The authors would like to thank Prof. Wolfgang Menzel from Ulm University for supporting far field measurements facilities. The authors would also appreciate Mr. Ralf Rudersdorfer, Mr. Bernhard Mayrhofer and Mr. Johann Katzenmayer from Johannes Kepler University Linz for their assistance in the manufacturing process.

References

[1] C. Wagner, H. Forstner, A. Stelzer, and H. Jaeger, “A 79-GHz single-chip radar transceiver with switchable TX and LO feedthrough in a silicon-germanium technology,” in IEEE Bipolar/BiCMOS Circuits and Technology Meeting Monterey, CA, accepted for publication,2008.

[2] T. Brauner, R. Vogt, and W. Baechtold, “A differential active patch antenna element for array applications,” IEEE Microwave and Wireless Components Letters, vol. 13, No 4, pp. 161-163, 2003.

[3] Y. P. Zhang, J. J. Wang, “Theory and analysis of differentially-driven microstrip antennas,” IEEE Trans. On Antennas and Propagation, vol. 54, No. 4, 2006.

[4] Constantine A. Balanis, *Antenna Theory: Analysis and Design*, 2nd edition, John Wiley & Sons. Inc., USA, pp.727-730, 1997.

[5] David E. Bockelman, William R. Eisenstadt, “Combined differential and common-mode scattering parameters: theory and simulation,” IEEE Tran. On Microwave Theory and Techniques, vol. 43, No. 7, pp.1530-1539, 1995.